Electronic Supplementary Material (ESI) for Dalton Transactions.

Coordination polymers from a highly flexible alkyldiamine-derived ligand: structure, magnetism and gas adsorption studies

Chris S. Hawes, Nicholas F. Chilton, Boujemaa Moubaraki, Gregory P. Knowles, Alan L. Chaffee, Keith S. Murray, Stuart R. Batten and David R. Turner

Supporting Information

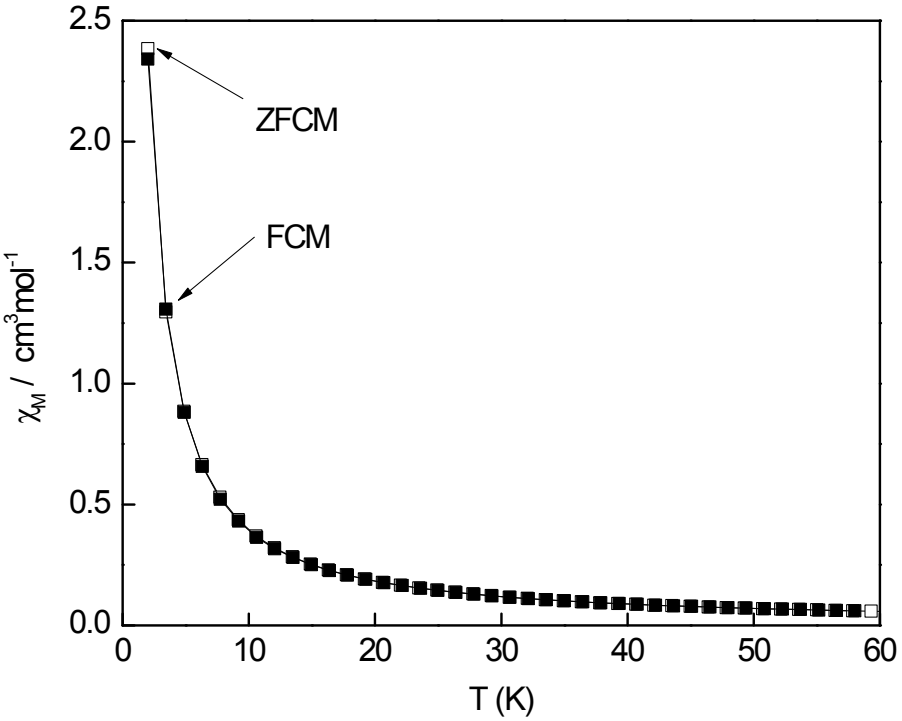

Figure S1 Plot of zero-field cooled magnetization (ZFCM, hollow squares) *versus* field cooled magnetization (FCM, filled squares) in the range 2 – 60K for compound **1**.

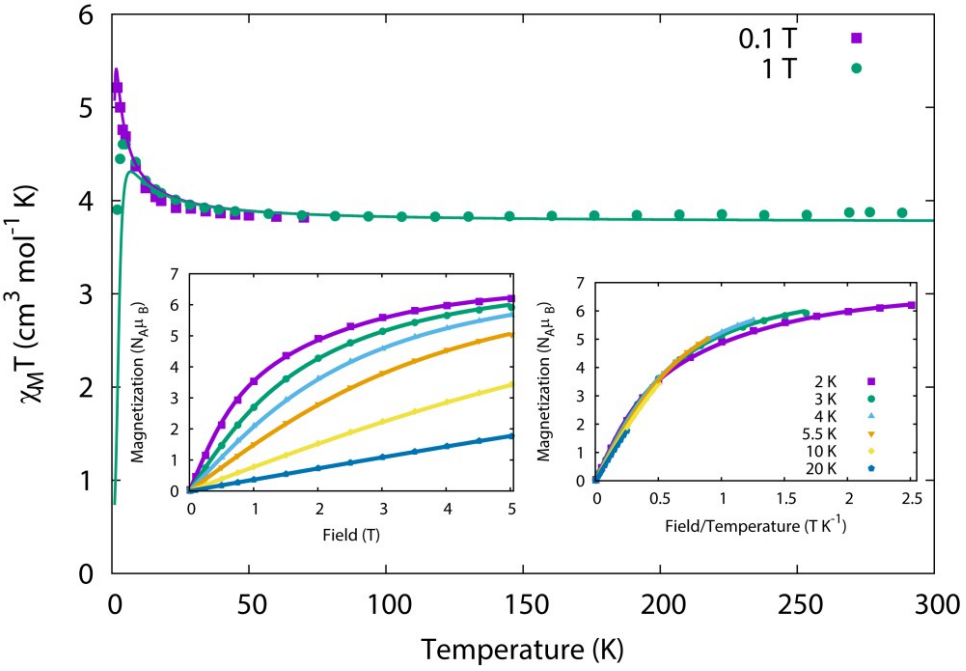

Figure S2 Plots of observed (solid points) and calculated (solid lines) χ_MT and magnetization (inset) for complex **1** with negative *D*, see text for best-fit parameters.

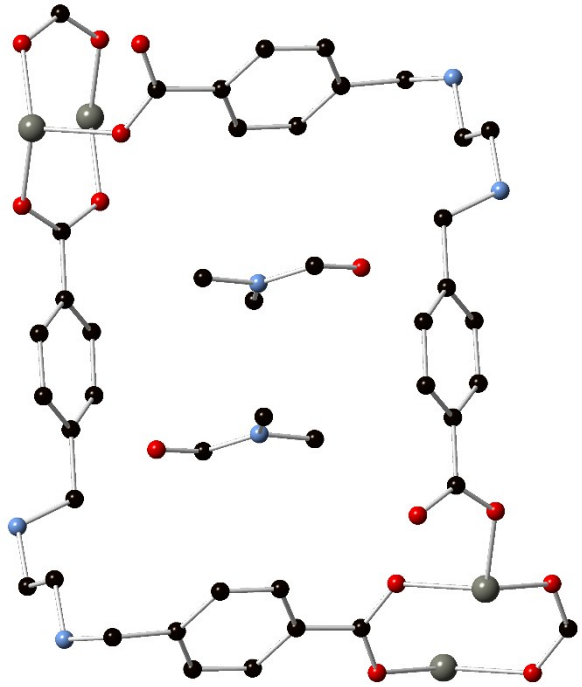

Figure S3 Encapsulated lattice DMF molecules within the structure of **2**. Hydrogen atoms and rotational disorder are omitted for clarity.

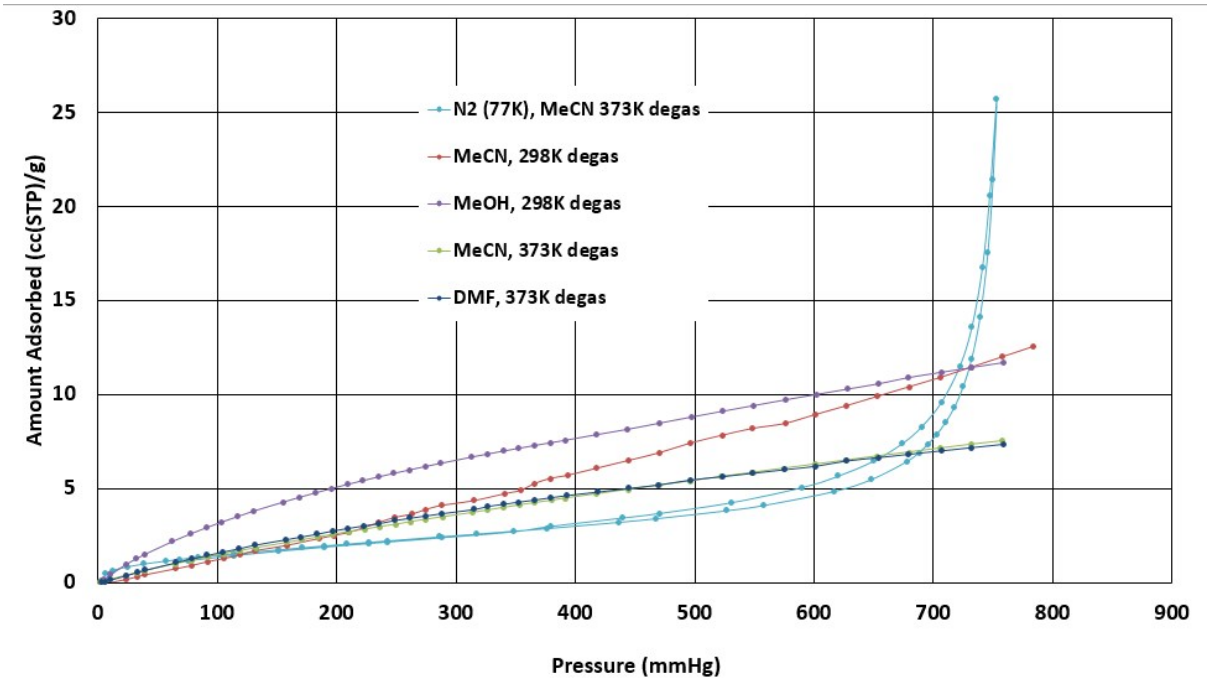

Figure S4 Overlaid gas adsorption isotherms (CO_2 adsorption at 273K, except where otherwise specified) for compound **2** and the solvent exchanged derivatives, with evacuation conditions as stated.

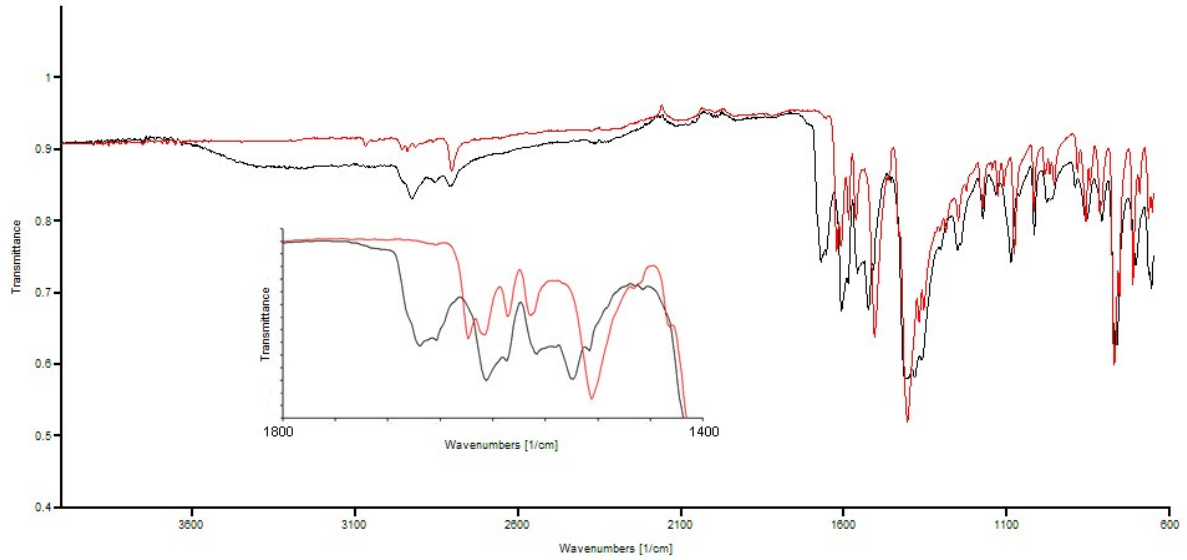

Figure S5 Overlaid FTIR spectra of the as-synthesised compound **2** (black) and compound **2** after framework desolvation and collapse (red). Inset: overlaid spectra in the frequency range 1800 – 1400 cm^{-1}, showing the loss of the absorbance due to lattice DMF (1662 cm^{-1}) and rearrangement of the remaining carbonyl absorbances suggesting an altered coordination mode upon framework collapse. Figure prepared using SpekWin32.[1]

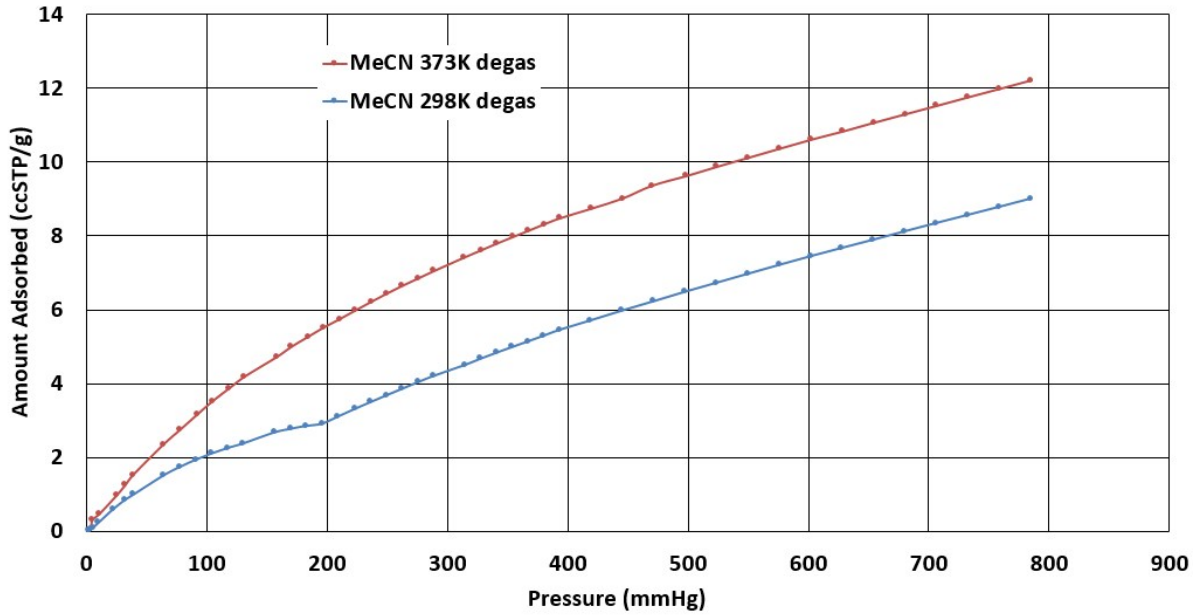

Figure S6 CO_2 adsorption isotherms for compound **3** following activation by acetonitrile exchange and evacuation at the specified temperatures, measured at 273K.

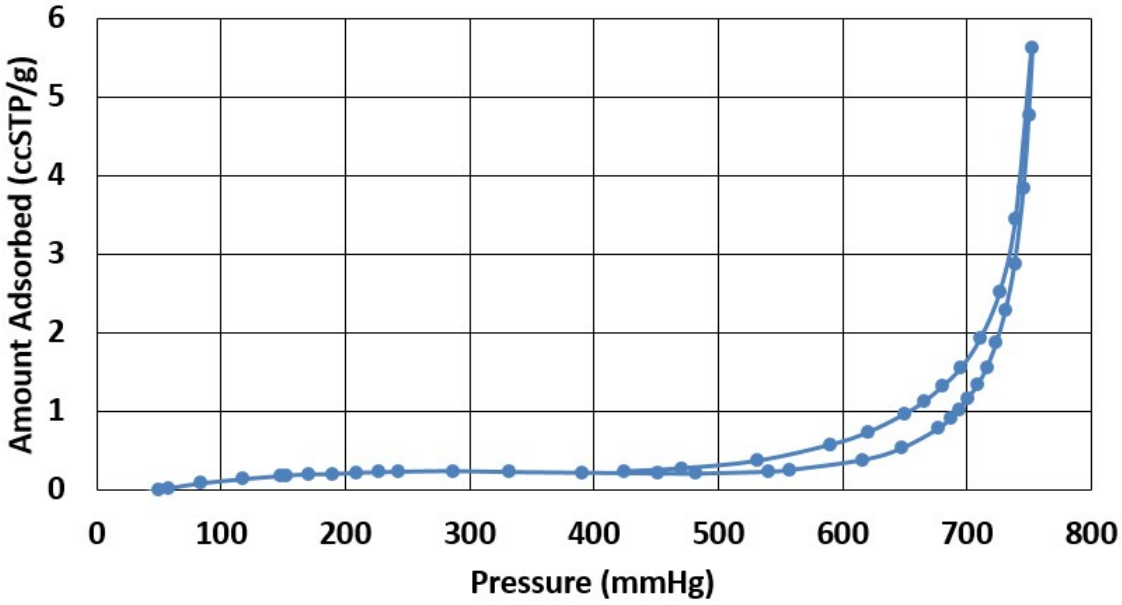

Figure S7 N_2 adsorption isotherm for compound **4** (MeCN exchanged and evacuated at 373K), measured at 77K.

Enthalpy of Adsorption Calculations for Compound 4

The isosteric heat of adsorption of CO_2 was calculated using a least-squares fitting of a virial thermal adsorption equation[2,3] which modelled ln(P) as a function of gas adsorbed over the measurement temperatures 273K and 302K, in the uptake range at which datapoints were recorded for both experiments (N = 0-1 mmol). The model function took the form $\ln(P) = \{\ln(N) + (a_0 + a_1N + a_2N^2)/T + b\}$ where N represents the surface excess adsorption of CO_2 in mmol at temperature T and $a_0 - a_2$ and b are coefficients determined through least squares fitting. The enthalpy of adsorption was then determined using the relation $Q(N) = -R(a_0 + a_1N + a_2N^2)$. Optimised virial coefficients and fitting parameters are given in the table below.

Table S1 Optimised virial coefficients and least squares fitting parameters for the CO_2 isotherms collected for compound **4**

Temperatures (K)	273, 302
a_0	-3536.86
a_1	-14.56
a_2	188.94
b	15.71
R^2	0.9990
Datapoints fitted	64

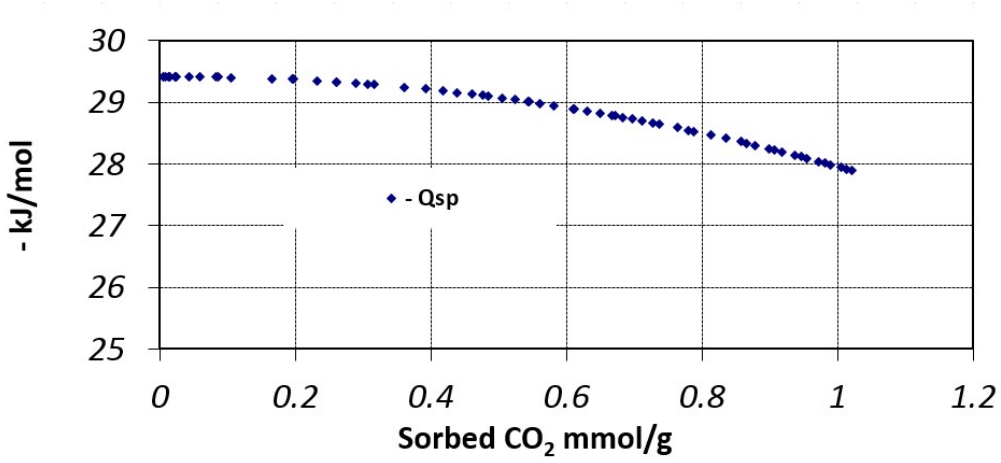

Figure S8 Enthalpy of adsorption as a function of CO_2 loading for compound **4**

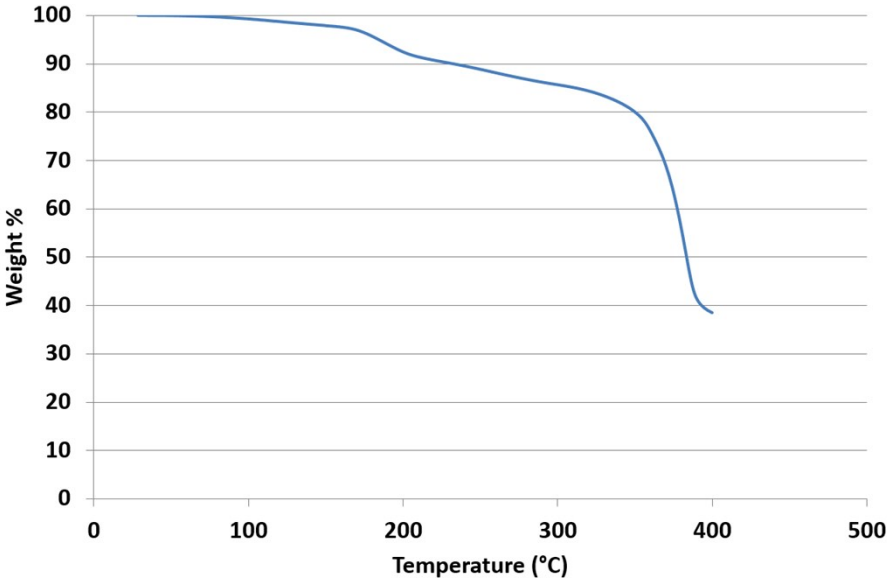

Figure S9 Thermogravimetric analysis for compound **1**

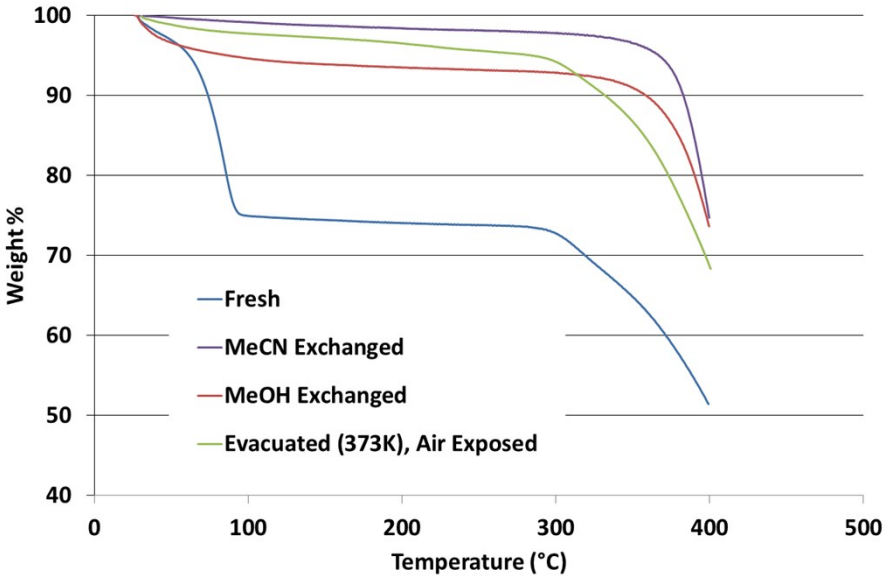

Figure S10 Thermogravimetric analysis plots for compound **2**, MeCN and MeOH exchanged compound **2**, and a sample of **2** dried by evacuating at 373K overnight and exposed to air for 72 hours.

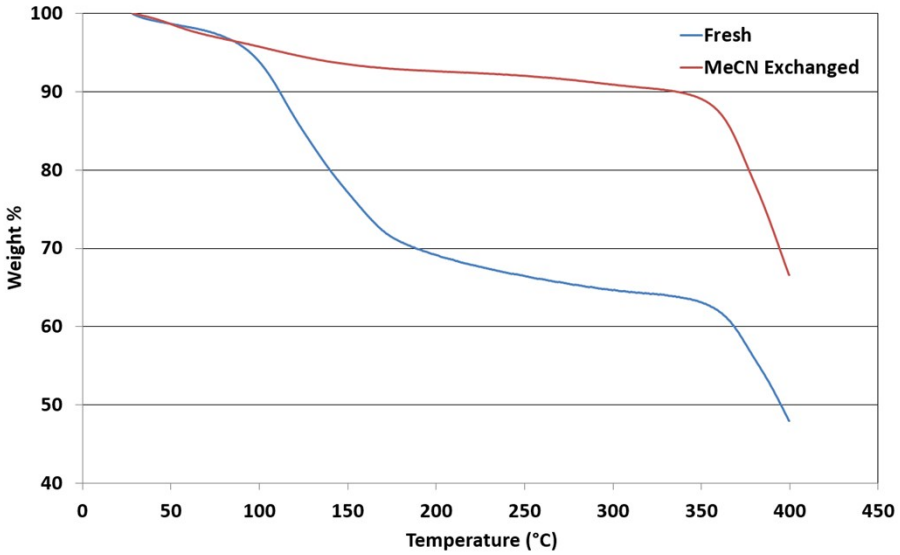

Figure S11 Thermogravimetric analysis plots for compounds **3** and the MeCN exchanged compound **3**.

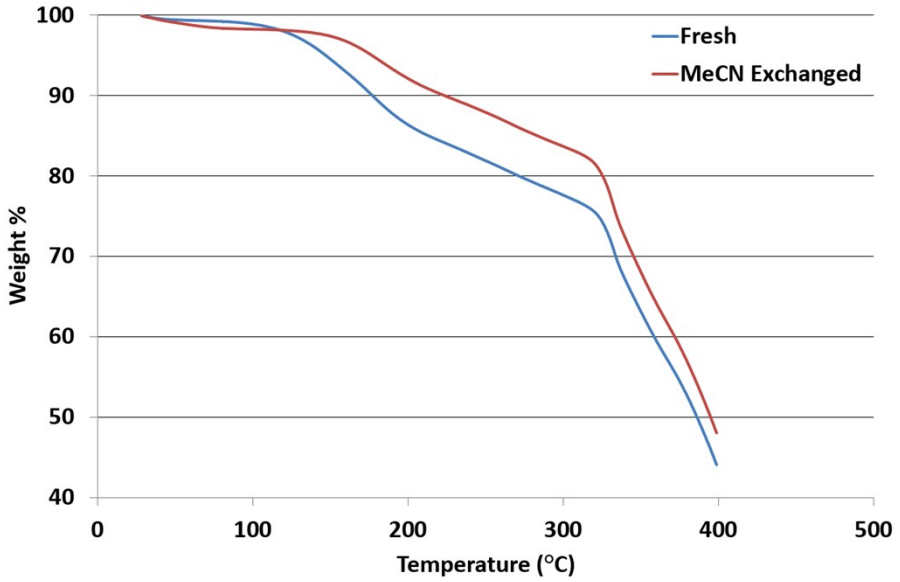

Figure S12 Thermogravimetric analysis plots for compound **4** and MeCN-exchanged compound **4**.

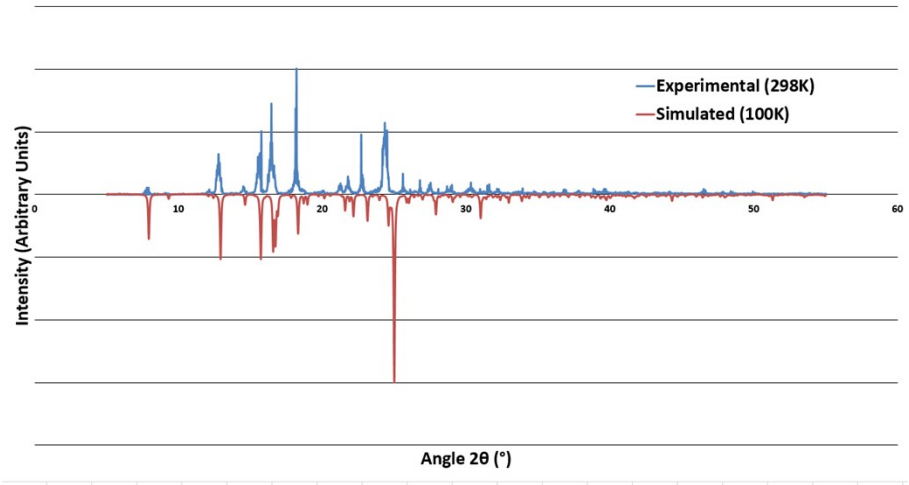

Figure S13 X-ray powder diffraction pattern for **H_4L**

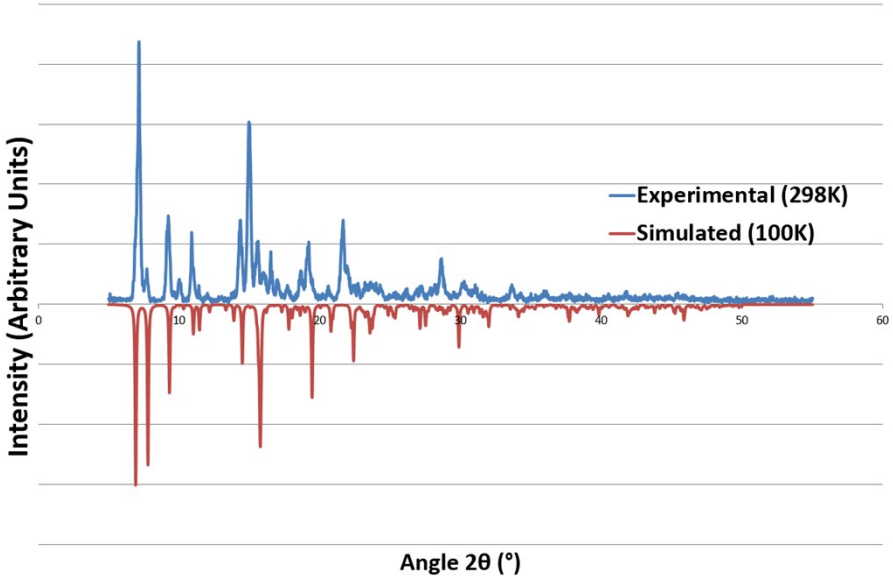

Figure S14 X-ray powder diffraction pattern for compound **1**. Due to the platelike morphology of the crystallites, the simulated pattern was modelled with preferred orientation [1,0,2].

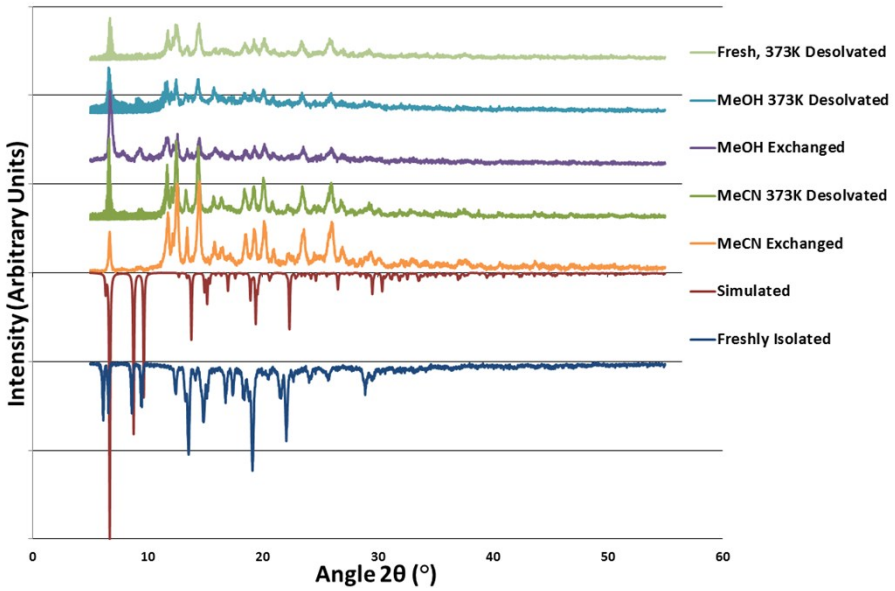

Figure S15 X-ray powder diffraction patterns for compound **2**, compared with patterns collected for the collapsed material obtained from solvent exchange and from direct thermal desolvation of the fresh material.

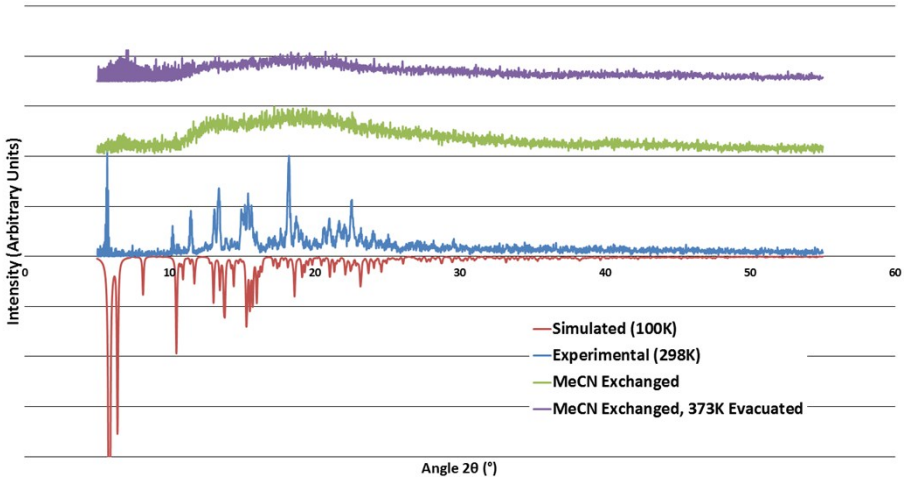

Figure S16 X-ray powder diffraction patterns for compound **3**, and the solvent-exchanged and evacuated materials.

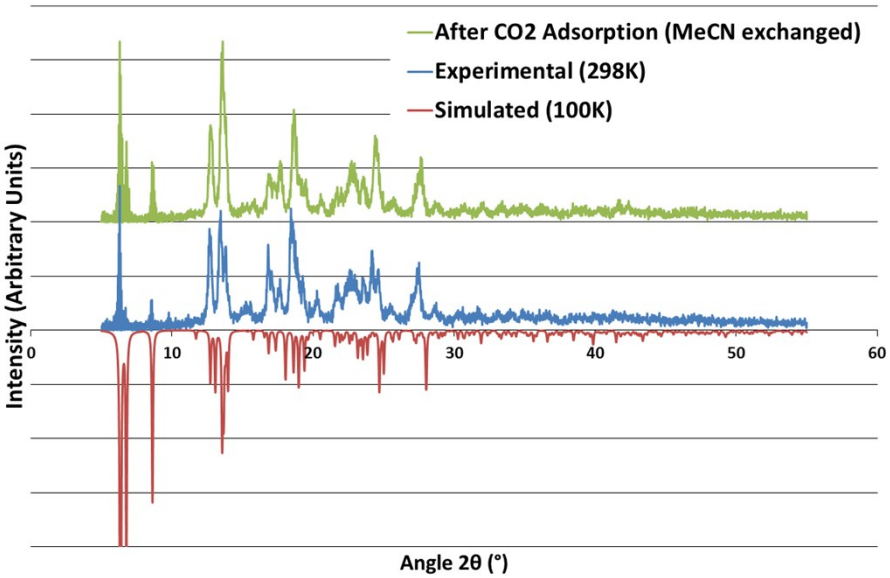

Figure S17 X-ray powder diffraction patterns for compound **4**, and compound **4** following solvent exchange, evacuation and gas adsorption studies.

Table S2 Hydrogen bonding parameters for **H_4L1** and compound **1**.

D	H	A	d(D-H)/Å	d(H-A)/Å	d(D-A)/Å	D-H-A/°
H_4L1						
O20	H20	O44[1]	0.880(15)	1.785(15)	2.6613(17)	174(2)
O1	H1	O34[2]	0.897(16)	1.703(16)	2.5987(17)	177(2)
O33	H33	O3[2]	0.914(16)	1.702(17)	2.6108(17)	172(2)
O43	H43	O21[1]	0.870(15)	1.723(16)	2.5926(17)	177(2)
[1]2-X,-Y,1-Z; [2]2-X,2-Y,-Z						
Compound **1**						
N13	H13	O50[1]	0.909(17)	1.91(2)	2.720(2)	147(3)
O47	H47A	O35[2]	0.848(17)	1.744(18)	2.5761(19)	167(3)
O47	H47B	O46[3]	0.848(17)	1.675(18)	2.5139(18)	170(3)
O48	H48A	O45[4]	0.843(18)	1.97(2)	2.7446(18)	153(3)
O48	H48B	O36	0.841(18)	2.04(2)	2.8168(18)	154(3)
[1]1-X,-Y,1-Z; [2]-X,1-Y,-Z; [3]-X,-Y,1-Z; [4]+X,1+Y,-1+Z						

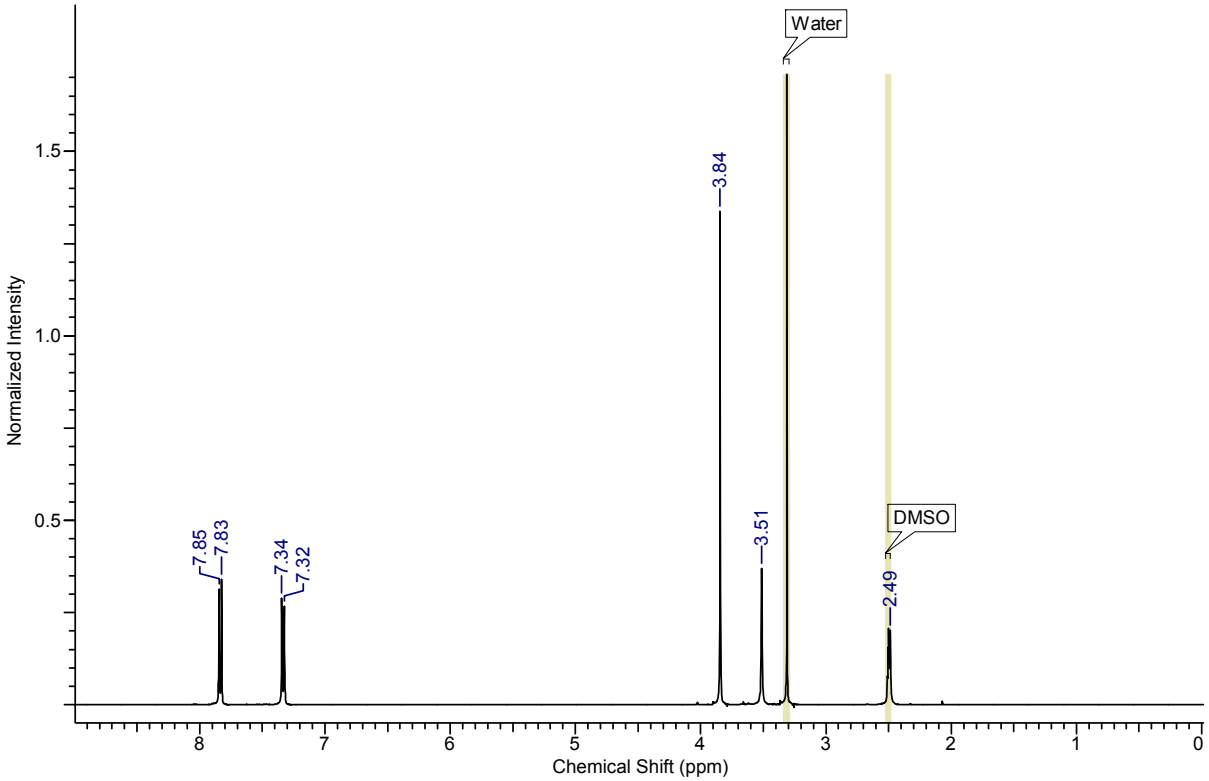

Figure S18 ^{1}H NMR Spectrum for **Me$_4$L**

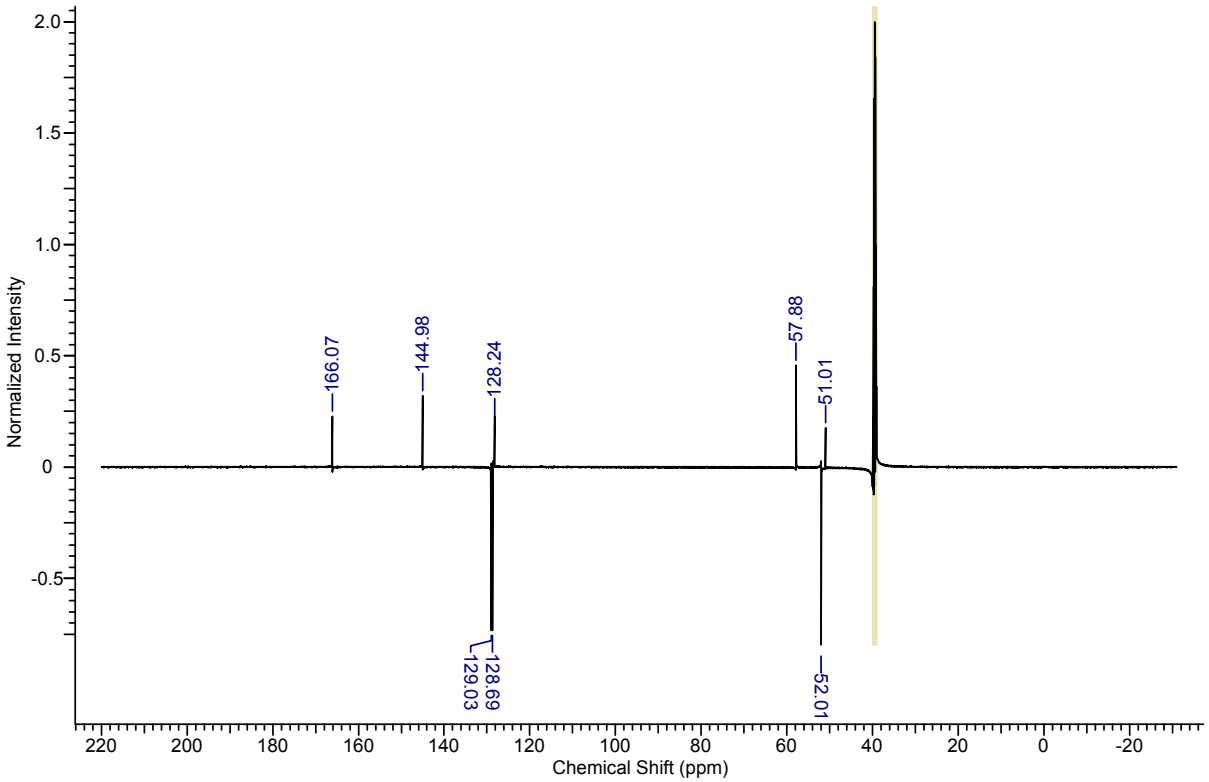

Figure S19 ^{13}C-DEPT spectrum for **Me$_4$L**

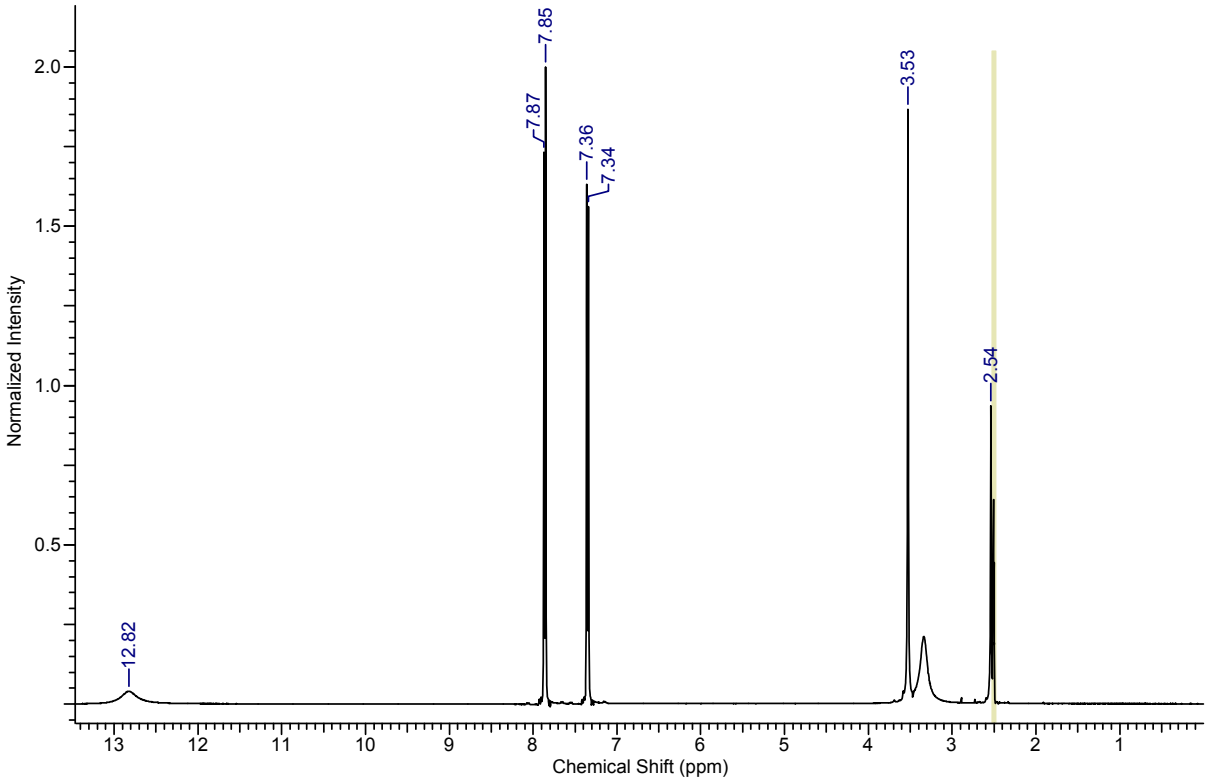

Figure S20 ^{1}H NMR spectrum for **H_4L**.

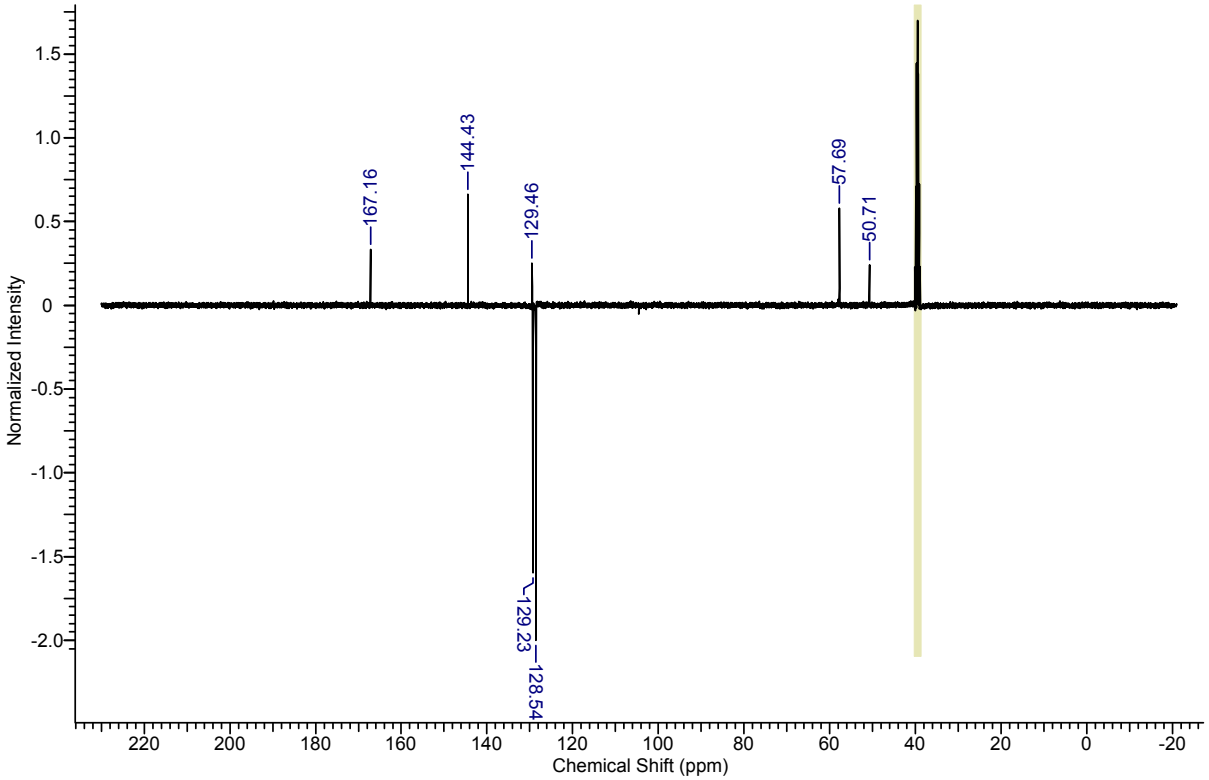

Figure S21 ^{13}C-DEPT Spectrum for **H_4L**

References

[1] F. Menges, *SpekWin32 – Optical Spectroscopy Software,* **Version 1.71.6.1***,* 2013

[2] Czepirski, L.; Jagiello, J. *Chem*. *Eng*. *Sci*. **1989**, *44*, 797-801.

[3] Tedds, S.; Walton, A.; Broom, D. P.; Book, D. *Faraday Discuss*. **2011**, *151*, 75-94.